the plant journal

SEB SOCIETY FOR EXPERIMENTAL BIOLOGY

The Plant Journal (2023) **115,** 627–641 doi: 10.1111/tpj.16250

HOS1 promotes plant tolerance to low-energy stress via the SnRK1 protein kinase

Leonor Margalha[†,*], Alexandre Elias[†], Borja Belda-Palazón[‡], Bruno Peixoto[§], Ana Confraria and Elena Baena-González[§,*]

Instituto Gulbenkian de Ciência, 2780-156 Oeiras, Portugal and GREEN-IT Bioresources for Sustainability, ITQB NOVA, 2780-157, Oeiras, Portugal

Received 21 February 2022; revised 5 April 2023; accepted 17 April 2023; published online 19 April 2023.
*For correspondence (e-mail leonor.margalha@itqb.unl.pt; elena.baena-gonzalez@biology.ox.ac.uk).
[†]These authors have equally contributed.
[‡]Present address: IBMCP-CSIC-UPV, 46022, Valencia, Spain
[§]Present address: Department of Biology, University of Oxford, South Parks Rd, Oxford OX1 3RB, UK

SUMMARY

Plants need to integrate internal and environmental signals to mount adequate stress responses. The NUCLEAR PORE COMPLEX (NPC) component HIGH EXPRESSION OF OSMOTICALLY RESPONSIVE GENES 1 (HOS1) is emerging as such an integrator, affecting responses to cold, heat, light, and salinity. Stress conditions often converge in a low-energy signal that activates SUCROSE NON-FERMENTING 1-RELATED KINASE 1 (SnRK1) to promote stress tolerance and survival. Here, we explored the role of HOS1 in the SnRK1-dependent response to low-energy stress in *Arabidopsis thaliana*, using darkness as a treatment and a combination of genetic, biochemical, and phenotypic assays. We show that the induction of starvation genes and plant tolerance to prolonged darkness are defective in the *hos1* mutant. HOS1 interacts physically with the SnRK1α1 catalytic subunit in yeast two-hybrid assays and *in planta*, and the nuclear accumulation of SnRK1α1 is reduced in the *hos1* mutant. Likewise, another NPC mutant, *nup160*, exhibits lower activation of starvation genes and decreased tolerance to prolonged darkness. Importantly, defects in low-energy responses in the *hos1* background are rescued by fusing SnRK1α1 to a potent nuclear localization signal or by sugar supplementation during the dark treatment. Altogether, this work demonstrates the importance of HOS1 for the nuclear accumulation of SnRK1α1, which is key for plant tolerance to low-energy conditions.

Keywords: HOS1, NUP160, nuclear pore complex, SnRK1, low-energy stress, *Arabidopsis thaliana*.

INTRODUCTION

Abiotic environmental stresses such as high and low temperature, drought, flooding, and salinity can be yield-limiting factors that compromise crop productivity. To cope with such adverse environmental conditions, plants have developed responses that promote stress tolerance and survival, usually at the expense of growth (Margalha et al., 2019).

The *HIGH EXPRESSION OF OSMOTICALLY RESPONSIVE GENE 1* (*HOS1*) locus was initially identified as a negative regulator of cold signaling in Arabidopsis (Dong et al., 2006; Ishitani et al., 1998; Lee et al., 2001). Subsequent studies unveiled the involvement of HOS1 in the response to other environmental signals, such as high temperature (Han et al., 2020; Zhang et al., 2020), light quality (Lazaro et al., 2015; MacGregor et al., 2013), and salinity (Zhu et al., 2017). HOS1 has been implicated in auxin (Lee & Seo, 2015a), ethylene (Lee & Seo, 2015b), and ABA signaling (Zhu et al., 2017), as well as in developmental processes such as germination (Lazaro et al., 2015), primary root growth (Zhu et al., 2017), hypocotyl elongation (Kim, Lee, Jung, et al., 2017; Kim, Lee, & Park, 2017; Lee & Seo, 2015a; MacGregor et al., 2013; Zhang et al., 2020), leaf expansion (Lee & Seo, 2015b; Zhang et al., 2020), and flowering (Jung et al., 2012; Jung et al., 2013; Lazaro et al., 2012; Lazaro et al., 2015; Lee et al., 2012; Seo et al., 2013).

HOS1 harbors a RING finger domain near the N-terminus of the protein (Lee et al., 2001) and acts as an E3 ubiquitin ligase promoting the proteasome-dependent degradation of the transcription factors INDUCER OF CBF EXPRESSION 1 (ICE1) (Dong et al., 2006) and CONSTANS (CO) (Lazaro et al., 2012), which are involved in cold acclimation and in the photoperiodic regulation of flowering, respectively. HOS1 also functions as a chromatin modifier, contributing to the transcriptional activation of the flowering repressor gene *FLOWERING LOCUS C* (*FLC*) (Jung

et al., 2013), the microRNA gene *MIR168b*, involved in *ARGONAUTE 1* (*AGO1*) regulation (Wang et al., 2015), and DNA repair genes such as *RECQ2*, encoding a DNA helicase important for thermotolerance (Han et al., 2020). Such functions are likely to be performed through association with chromatin binding factors since a direct association with DNA has not been demonstrated. In these cases, as well as in the case of the transcription factor PHYTOCHROME INTERACTING FACTOR 4 (PIF4), HOS1 modulates protein function through mechanisms that do not involve proteasomal degradation (Han et al., 2020; Jung et al., 2013; Kim, Lee, Jung, et al., 2017; Lee et al., 2012). On the other hand, HOS1 is the only protein encoded by the Arabidopsis genome with a region of homology to the yeast and animal nucleoporin (NUP) ELYS (Jung et al., 2014). HOS1 interacts directly with the nuclear pore complex (NPC) components NUP96 (Cheng et al., 2020) and NUP160 (Li et al., 2020) and co-immunopurifies with RAE1, NUP43 (Tamura et al., 2011), and NUP85 (Zhu et al., 2017). With the exception of RAE1, all the mentioned NUPs belong to the NUP107-160 subcomplex, the major constituent of the outer ring complex of the NPC core scaffold, with essential structural functions (Li & Gu, 2020). These interactions support a role for HOS1 in the NPC-mediated control of nucleo-cytoplasmic trafficking. In line with such role, *hos1* plants show nuclear retention of polyadenylated mRNAs, which may underlie the lengthened circadian period observed in this mutant (MacGregor et al., 2013). In addition, nuclear accumulation of the PIF4 transcription factor is reduced in *hos1*, compromising the response of the mutant to warm temperatures (Zhang et al., 2020). Several other *nup* mutants are, like *hos1*, also affected in mRNA export and nucleo-cytoplasmic trafficking of proteins, temperature signaling, circadian function, plant growth, and flowering time (MacGregor & Penfield, 2015; Zhang et al., 2020).

Most types of environmental stress compromise photosynthesis or/and respiration (Cho et al., 2021; Muhammad et al., 2021), thereby leading to reduced ATP production and low-energy stress (Branco-Price et al., 2008; de Col et al., 2017; Tomé et al., 2014). One major player in the sensing of energy resources and the orchestration of adequate downstream responses is the evolutionarily conserved SUCROSE NON-FERMENTING 1 (SNF1)-RELATED KINASE 1 (SnRK1), the plant ortholog of mammalian AMP-ACTIVATED KINASE (AMPK) and yeast SNF1. SnRK1 is activated when energy levels decline and is repressed by sugars such as trehalose 6-phosphate, glucose 6-phosphate, and glucose 1-phosphate (Nunes et al., 2013; Peixoto et al., 2021; Zhai et al., 2018; Zhang et al., 2009). Upon activation, SnRK1 drives vast transcriptional and metabolic adjustments to stimulate energy-producing catabolic processes and inhibit energy-consuming biosynthetic processes and growth (Baena-González et al., 2007; Baena-González & Sheen, 2008; Cho et al., 2012; Pedrotti et al., 2018). Constitutive manipulation of SnRK1 levels results in altered tolerance to a wide range of stresses (Hulsmans et al., 2016; Margalha et al., 2019) and affects multiple aspects of growth and development (Baena-González & Hanson, 2017; Jamsheer et al., 2021).

Like its mammalian and yeast orthologs, SnRK1 functions as a heterotrimeric complex composed of a catalytic α-subunit and regulatory β- and γ-subunits, encoded by different genes (*SnRK1α1*/*α2*, *SnRK1β1*/*β2*/*β3*, and *SnRK1βγ* in Arabidopsis). Despite the functional and structural conservation, SnRK1 displays unique features that may underlie functions and modes of regulation specific to plants (Broeckx et al., 2016; Emanuelle et al., 2015; Ramon et al., 2013). Recent studies have highlighted the importance of subcellular localization for SnRK1 function, with clear phenotypes associated with the confinement of SnRK1 inside or outside of the nucleus (Gutierrez-Beltran & Crespo, 2022; Ramon et al., 2019). The nuclear localization of SnRK1 is essential for its role in transcriptional regulation and is promoted by stresses that cause an energy deficit, although this response may be limited to specific cell types or tissues (Blanco et al., 2019; Cho et al., 2012; Ramon et al., 2019). The nuclear localization of SnRK1 responds also to N (Sun et al., 2021; Yuan et al., 2016) and to ABA signaling (Belda-Palazón et al., 2022) and displays a diurnal oscillation pattern (Yuan et al., 2016). On the other hand, SnRK1 phosphorylates metabolic enzymes (e.g., SUCROSE PHOSPHATE SYNTHASE [SPS] and NITRATE REDUCTASE [NR]; Nukarinen et al., 2016; Sugden et al., 1999) that reside outside the nucleus. SnRK1 was also found to associate with the ER (Blanco et al., 2019), where it interacts with FCS-like zinc finger (FLZ) proteins (Jamsheer et al., 2018), and with the ER perinuclear ring (Blanco et al., 2019), where it co-localizes with a component of the TARGET OF RAPAMYCIN (TOR) complex, REGULATORY ASSOCIATED PROTEIN OF TOR 1B (RAPTOR1B) (Nukarinen et al., 2016). However, the mechanisms that regulate the subcellular distribution of SnRK1 are poorly understood.

In this study we show that HOS1 is important for plant tolerance to low-energy conditions and that this is largely due to its involvement in the accumulation of SnRK1α1 in the nucleus.

RESULTS

HOS1 is required for low-energy responses

HOS1 is a multifaceted protein with a central role in diverse stress responses (MacGregor & Penfield, 2015). Given that numerous stress conditions lead to low energy levels (Baena-González & Sheen, 2008; Tomé et al., 2014), we wondered whether HOS1 could be involved in the response to low-energy stress. To investigate this, we compared the induction of starvation genes by reverse

transcription quantitative PCR (RT-qPCR) in leaves of wild-type Columbia-0 (Col-0) and the *hos1-3* knockout mutant (hereafter referred to as *hos1*; Lazaro et al., 2012) in response to a 3-h dark treatment. Starvation genes are involved in metabolic rearrangements and nutrient remobilization strategies and are essential for coping with low-energy stress (Baena-González et al., 2007; Baena-González & Sheen, 2008; Cookson et al., 2016; Pedrotti et al., 2018; Ramon et al., 2019). As shown in Figure S1, a 3-h dark treatment was sufficient to activate starvation genes such as *DIN6*, *DIN1*, and *DRM2* in Col-0 but the induction of these genes was reduced in the *hos1* mutant (Figure S1a). These defects were partially rescued in the *35S::HOS1-GFP*/*hos1* line *13–9* (hereafter referred to as *HOS1-GFP*, Figure S1a,d). These results suggested the involvement of HOS1 in the response to low-energy stress.

Successful activation of starvation genes is associated with survival after prolonged periods of darkness (Pedrotti et al., 2018). We therefore tested whether the inability of *hos1* to mount an adequate starvation response at the molecular level led to decreased plant tolerance to prolonged dark stress. To this end, we transferred 4-week-old plants to darkness for 7 days and placed them back in the light for 7 days to recover. In agreement with the molecular response to 3-h dark treatments, *hos1* plants showed decreased tolerance to prolonged darkness, manifested as yellowing and wilting of the leaves at 7 days (Figure S1b) and as compromised growth or complete growth arrest during the subsequent recovery period (7 + 7 days) (Figure S1b). The differences in the sensitivity to prolonged darkness between Col-0 and *hos1* were also reflected in the gain in rosette fresh weight determined at 7 days and at 7 + 7 days as compared to day 0 (Figure S1c). Furthermore, the decreased plant tolerance of *hos1* was partially reverted in the *HOS1-GFP* complementation line (Figure S1b,c). A different mutant allele of *HOS1*, *hos1-4* (Lazaro et al., 2012), was also analyzed (Figure S2). To better monitor the molecular response to prolonged dark treatment, samples were collected 2 days after the onset of darkness. Similarly to *hos1-3* (Figure S1), *hos1-4* plants showed defective induction of starvation genes (Figure S2a) and decreased plant tolerance (Figure S2b), with a lower gain in rosette fresh weight than Col-0 after the dark treatment (Figure S2c). Altogether, these results support a role for HOS1 in plant tolerance to prolonged darkness.

Starvation genes are under the control of the SnRK1 protein kinase, which is activated in response to low-energy conditions and repressed by sugars (Baena-González et al., 2007; Baena-González & Sheen, 2008; Pedrotti et al., 2018; Ramon et al., 2019). SnRK1 is also required for surviving prolonged periods of darkness (Henninger et al., 2022; Pedrotti et al., 2018; Ramon et al., 2019). To investigate if the defects of *hos1* in low-energy signaling are SnRK1-dependent, we crossed *hos1* to a *SnRK1α1* loss-of-function mutant, *snrk1α1–3* (hereafter referred to as *snrk1α1*; Crozet et al., 2016; Mair et al., 2015), and assessed the response of the double mutant to darkness. The 2-day dark treatment led to defective induction of starvation genes in *hos1* (Figure 1a) and in the *snrk1α1* mutant, confirming previous reports that this response is SnRK1-dependent (Henninger et al., 2022; Pedrotti et al., 2018; Ramon et al., 2019). However, *snrk1α1* plants displayed only a mild sensitivity to prolonged darkness (Figure 1b,c). This is in agreement with the functional redundancy between the two catalytic α-subunits of SnRK1, encoded by the *SnRK1α1* and *SnRK1α2* genes in Arabidopsis (Baena-González et al., 2007; Ramon et al., 2019). The *hos1*/*snrk1α1* double mutant showed defects in the induction of starvation genes that were either similar to defects in the *snrk1α1* and *hos1* parents or slightly enhanced (Figure 1a). The sensitivity of *hos1*/*snrk1α1* to prolonged darkness was similar to that of *hos1*, both being severely compromised or unable to resume growth during the 7-day recovery period (Figure 1b,c). Overall, these results suggest that HOS1 is required for adequate SnRK1 signaling in response to low-energy stress.

To further determine if *hos1* sensitivity to prolonged darkness resulted indeed from the ensuing energy deprivation, Col-0 and *hos1* plants were grown on 0.5× MS media plates with or without 1% sucrose and subjected to prolonged dark treatment (Figure S3). In agreement with a role for HOS1 in the low-energy stress response, sugar supplementation could largely rescue the sensitive phenotype of *hos1* at 7 + 7 days and increase the survival rate of *hos1* seedlings from 29% in control medium to 100% in the presence of sugar (Figure S3a,b).

Nuclear accumulation of SnRK1α1 requires HOS1

We next performed protein–protein interaction studies to investigate whether the requirement for HOS1 for proper SnRK1 signaling could be based on a physical interaction between HOS1 and SnRK1α1 (Figure 2). In yeast two-hybrid (Y2H) assays, cell growth in highly stringent media was only observed when both proteins were co-expressed (Figure 2a), indicating a direct interaction between SnRK1α1 and HOS1 in yeast cells. To assess if SnRK1α1 interacts with HOS1 also *in planta*, we performed co-immunoprecipitation (co-IP) experiments, pulling down GFP from *HOS1-GFP* or *GFP* control plants. Subsequent Western blot (WB) detection with an antibody against SnRK1α1 showed that SnRK1α1 co-purified with HOS1-GFP but not with GFP alone (Figure 2b).

Given the physical interaction between HOS1 and SnRK1α1, we next asked if HOS1 could affect SnRK1 stability. HOS1 has an E3 ubiquitin ligase activity that is key for many environmental and developmental responses (Dong et al., 2006; Jung et al., 2012; Lazaro et al., 2012; Lazaro et al., 2015; Lee et al., 2012). Furthermore, HOS1 and the

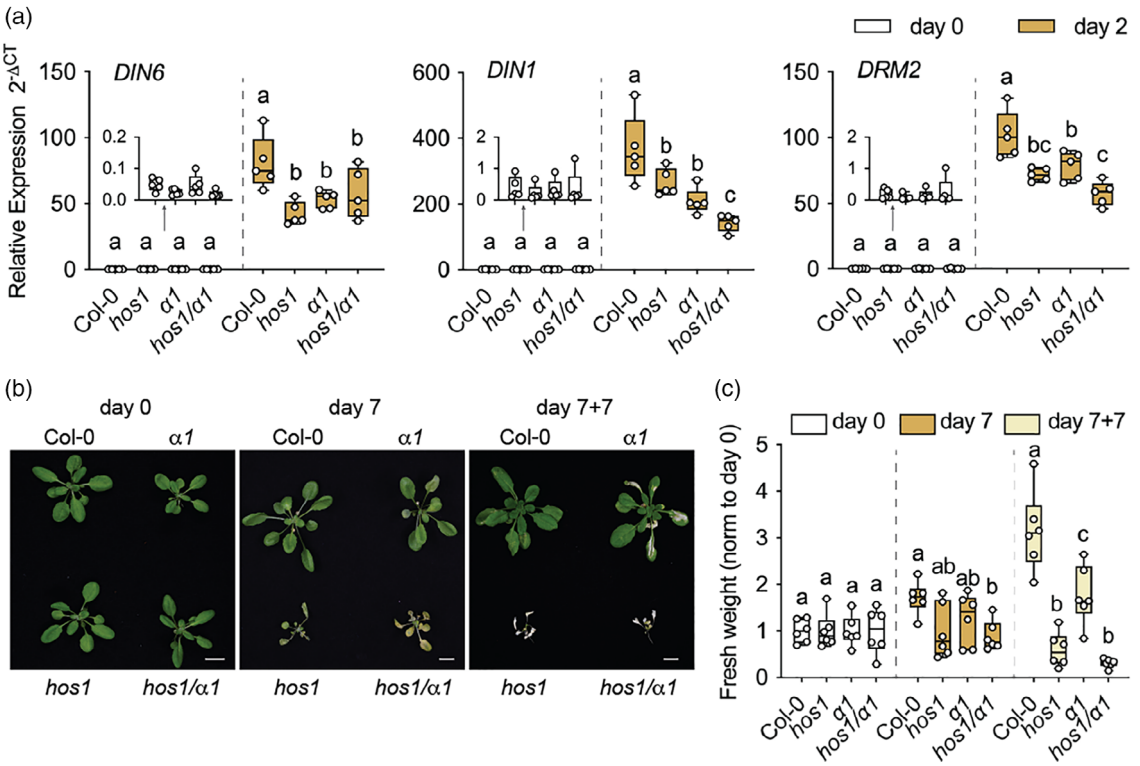

Figure 1. Tolerance of *hos1* and *snrk1α1* mutants to prolonged darkness. (a) Induction of starvation genes (*DIN6*, *DIN1*, *DRM2*) measured by RT-qPCR from rosettes of Col-0, *α1* (*snrk1α1*), *hos1*, and *hos1*/*α1* plants collected on day 0 and after 2 days of dark treatment (day 2). Box and whisker plots represent five biological replicates (each consisting of one rosette per genotype and condition, grown in five independent batches). (b) Representative pictures of 4-week-old plants (day 0) of the indicated genotypes placed in constant darkness for 7 days (day 7) and transferred back to the initial photoperiod for 7 additional days (day 7 + 7). Scale bar = 1 cm. (c) Rosette fresh weight determined on days 0, 7, and 7 + 7 and normalized to day 0 for each genotype. Box and whisker plots represent six plants per genotype and condition (grown in three independent batches). Different letters denote statistically significant differences between genotypes within each condition (days 0, 2, 7, and 7 + 7), as determined by two-way ANOVA with Tukey's multiple comparisons test ($P < 0.05$).

SUMO E3 ligase SIZ1 act antagonistically on ICE1 stability (Miura et al., 2007; Miura et al., 2011), and SIZ1 has been implicated in the SUMO-dependent proteasomal degradation of SnRK1 (Crozet et al., 2016). However, no clear differences were observed in total protein extracts between Col-0 and *hos1* regarding the accumulation of the SnRK1α1 and SnRK1α2 catalytic subunits, their T-loop phosphorylation, necessary for kinase activity (Baena-González et al., 2007; Shen et al., 2009), or the levels of the SnRK1β1 regulatory subunit (Figure S4). These results suggest that the increased sensitivity of *hos1* in response to prolonged darkness is unrelated to changes in total SnRK1 protein accumulation.

HOS1 localization at the NPC is essential for some of its functions (Li et al., 2020). On the other hand, the activation of starvation genes by SnRK1 requires its presence in the nucleus (Cho et al., 2012; Ramon et al., 2019). Therefore, we asked whether HOS1 could affect specifically the nuclear pool of SnRK1α1. To test this, we performed nuclear fractionation from Col-0 and *hos1* rosettes and analyzed SnRK1α1 in the resulting fractions (Figure 3). No significant differences were observed in SnRK1α1 levels in the cytoplasmic fractions of Col-0 and *hos1* (Figure 3a,b). However, the protein levels of SnRK1α1 were reduced in the nuclear fraction of *hos1* in comparison to Col-0 (Figure 3a,b). A lower accumulation of SnRK1α1 in the nucleus of *hos1* was also observed after a 9-h dark treatment (Figure 3c,d), reported to induce nuclear translocation of SnRK1α1 (Ramon et al., 2019), indicating that HOS1 is important for the accumulation of SnRK1α1 in the nucleus both under control and low-energy conditions.

These data suggested a constitutive effect of HOS1 on the nuclear accumulation of SnRK1α1. To investigate if this effect is associated with the NPC localization or function of HOS1, we examined the response to low-energy stress in the *nup160* mutant (Figure 4) since the NUP160 subunit is required for anchoring HOS1 at the NPC (Li et al., 2020). Similarly to *hos1*, *nup160* showed defective activation of starvation genes in response to 2 days of darkness (Figure 4a), decreased plant tolerance to an extended 7-day period of darkness, and a compromised ability to resume growth in the subsequent recovery period (Figure 4b,c). This suggests that anchoring HOS1 at the NPC, or NPC integrity, is important for nuclear

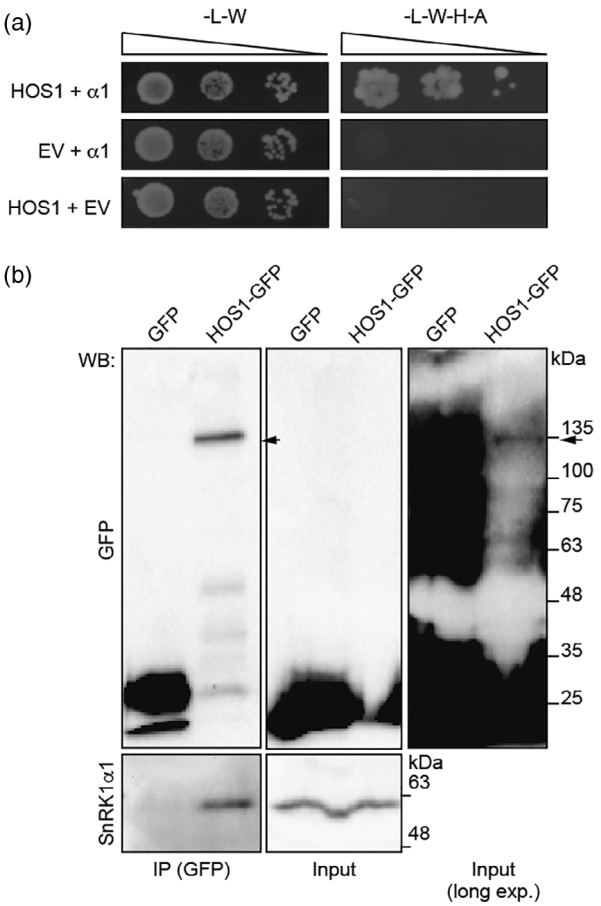

Figure 2. Physical interaction between HOS1 and SnRK1α1. (a) Yeast two-hybrid assays. Yeast cell growth after expression of HOS1 and SnRK1α1 (α1), together or alone with the complementary empty vectors (EV), in low- (−L/−W) or high-stringency (−L/−W/−H/−A) medium. L, leucine; W, tryptophan; H, histidine; A, adenine. Representative image of three biological replicates, grown in three independent batches. (b) GFP immunoprecipitation (IP) from rosettes of 4-week-old *35S::GFP* (*GFP*) or *35S::HOS1-GFP*/*hos1* (*HOS1-GFP*) plants. WB with antibodies against GFP and SnRK1α1. Right panel, longer exposure of the middle panel to visualize HOS1-GFP in the input. Black arrows point to HOS1-GFP. Representative image of three biological replicates (each consisting of one rosette per genotype, grown in three independent batches).

accumulation of SnRK1α1 and for an adequate starvation response. Moreover, a double *nup160*/*hos1* mutant showed a similar plant phenotype upon prolonged darkness to the single mutant parents (Figure S5), supporting that the two nucleoporins act in the same pathway to promote tolerance to low-energy stress.

Fusion of SnRK1α1 to a potent nuclear localization signal rescues *hos1* defects in low-energy responses

We next wondered if depletion of SnRK1α1 from the nucleus (Figure 3a–d) was sufficient to explain the molecular and plant phenotypes of *hos1* in response to darkness (Figure 1; Figures S1, S3, and S5). To assess this, we crossed the *hos1* mutant to two recently described lines, in which the *snrk1α1*/*snrk1α2* double mutant was complemented with SnRK1α1 variants with different subcellular localizations (Ramon et al., 2019). In one line, the simian virus 40 large T-antigen nuclear localization signal (NLS) (SV40-NLS) was fused N-terminally to SnRK1α1 to increase its nuclear localization (Figure 5, *NLS-α1* [*NLS-SnRK1α1*/*snrk1α1*/*snrk1α2*]). In the other line, the N-terminal myristoylation motif of the SnRK1β2 subunit was fused N-terminally to SnRK1α1 to increase its membrane association and exclusion from the nucleus (Figure 5, *βMYR-α1* [*βMYR-SnRK1α1*/*snrk1α1*/*snrk1α2*]). Nuclear fractionation from *hos1* and *hos1*/*NLS-α1* (*NLS-SnRK1α1*/*snrk1α1*/*snrk1α2*/*hos1*) plants showed that fusing the SV40-NLS motif to SnRK1α1 can indeed increase its nuclear accumulation in the *hos1* background (Figure 5a,b). Most importantly, the *NLS-SnRK1α1* transgene in the *hos1*/*NLS-α1* plants was able to restore normal induction of starvation genes in response to darkness (Figure 5c) and rescue to a large extent the *hos1* sensitivity to the 7-day dark treatment and recovery (Figure 5d), with a significant increase in the fresh weight gain in the *hos1*/*NLS-α1* line in comparison to *hos1* (Figure 5e). By contrast, the *βMYR-SnRK1α1* transgene in *hos1*/*βMYR-α1* plants (*βMYR-SnRK1α1*/*snrk1α1*/*snrk1α2*/*hos1*) aggravated the defects of *hos1* in the induction of starvation genes in response to darkness (Figure 5c). Consequently, expression of *βMYR-SnRK1α1* exacerbated the sensitivity of *hos1* to prolonged dark treatment (Figure 5d,e). Collectively, these results suggest that the molecular and plant phenotypes of *hos1* in response to low-energy conditions are at least partially caused by the reduced nuclear accumulation of SnRK1α1.

To investigate the specificity of the restorative effects of the *NLS-SnRK1α1* transgene on *hos1* phenotypes, we also monitored flowering time, since both HOS1 (Jung et al., 2012; Jung et al., 2013; Lazaro et al., 2012; Lee et al., 2012; Seo et al., 2013) and SnRK1α1 (Baena-González et al., 2007; Jeong et al., 2015; Sanagi et al., 2021; Tsai & Gazzarrini, 2012; Williams et al., 2014) were shown to act as negative regulators of this trait. However, the early flowering phenotype of *hos1* in long-day conditions was not modified by changes in SnRK1α1 localization, with both *hos1*/*NLS-α1* and *hos1*/*βMYR-α1* plants showing early flowering similar to *hos1* (Figure S6). This indicates that not all *hos1* phenotypes can be complemented by enhancing the levels of SnRK1α1 in the nucleus.

DISCUSSION

Since its first identification as a negative regulator of cold signaling, the role of HOS1 has expanded towards the integration of environmental and endogenous signals in numerous stress and developmental responses (Dong et al., 2006; Han et al., 2020; Ishitani et al., 1998; Lazaro et al., 2012; Lazaro et al., 2015; Lee et al., 2001; Lee et al.,

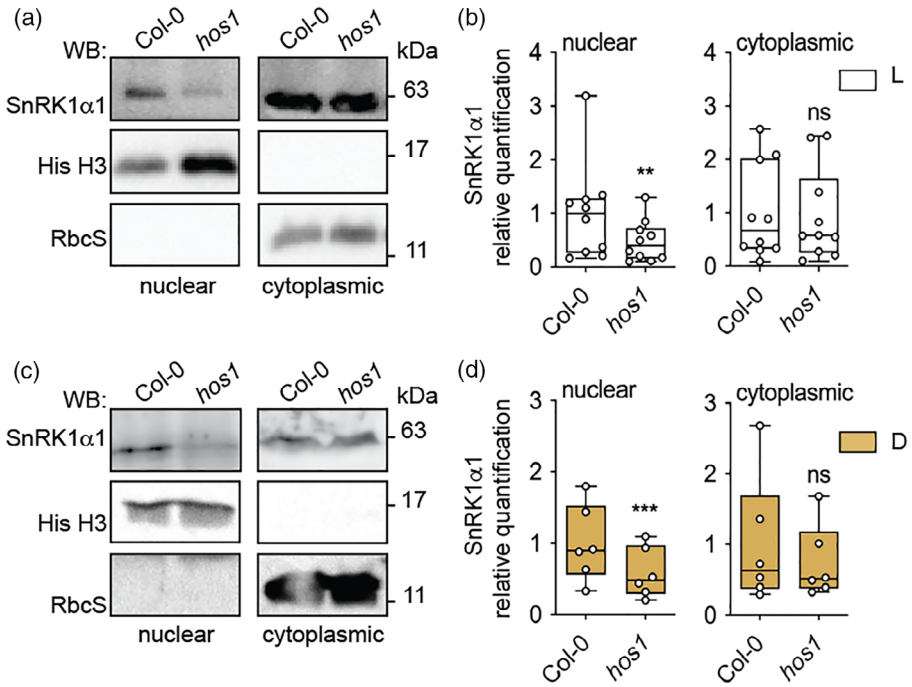

Figure 3. Nuclear accumulation of SnRK1α1 in *hos1*. (a–d) Nuclear fractionation from rosettes of 4-week-old Col-0 and *hos1* plants under control light (L) conditions (a, b) or after a 9-h dark (D) extension (c, d). (a, c) Representative WB of nuclear and cytoplasmic fractions with antibodies against SnRK1α1, histone 3 (His H3, nuclear marker, not detected in the WB image of the cytoplasmic fraction), and Rubisco small subunit (RbcS, cytosolic marker, not detected in the WB image of the nuclear fraction). (b, d) SnRK1α1 quantification normalized to His H3 in the nuclear fraction and to RbcS in the cytoplasmic fraction and further normalized to Col-0. Box and whisker plots represent a minimum of six biological replicates (each consisting of one rosette per genotype and condition, grown in a minimum of six independent batches). Asterisks denote statistically significant differences between Col-0 and *hos1*, as determined by a ratio paired *t*-test. $^{**}P < 0.01$; $^{***}P < 0.001$; *ns*, non-significant.

2012; Lee & Seo, 2015a; Lee & Seo, 2015b; MacGregor et al., 2013; Zhang et al., 2020; Zhu et al., 2017). Here, we identify HOS1 as a positive regulator of the low-energy stress response triggered by unexpected or prolonged darkness (Figure 6).

The *hos1* mutants displayed defective induction of starvation genes (Figures S1a and S2a, Figures 1a and 5c) and increased sensitivity to prolonged darkness (Figures S1b,c and S2b,c, Figures 1b,c and 5d,e). Importantly, sugar supplementation could rescue the *hos1* sensitive phenotype (Figure S3a,b), likely by counteracting the impact of darkness on cellular energy levels and hence offsetting the need to induce an adequate starvation response (Baena-González et al., 2007). Supporting this view, *hos1* plants showed no symptoms of low-energy stress under control conditions, where photosynthesis and respiration are not limited (Figure 1, day 0). Responses to low-energy conditions are under control of the SnRK1 signaling pathway, whose main components are the SnRK1 protein kinase and the C- and S-subclasses of bZIP transcription factors (Baena-González et al., 2007; Dröge-Laser & Weiste, 2018; Mair et al., 2015; Pedrotti et al., 2018). Although we did not test specifically for defects in bZIP transcription factors, our data suggest that the defect of the *hos1* mutants in low-energy signaling is at least in part related to the SnRK1 kinase itself. Firstly, we show that HOS1 promotes tolerance to low-energy conditions (Figure 1; Figures S1 and S2). Secondly, we show that it interacts physically with SnRK1α1 (Figure 2) and that *hos1* exhibits reduced accumulation of nuclear SnRK1α1 (Figure 3). Finally, we show that promoting the nuclear accumulation of SnRK1α1 in *hos1* through an NLS rescues to a large extent the defects of the *hos1* mutant in low-energy responses (Figure 5).

HOS1 has an E3 ubiquitin ligase activity that was shown to promote proteasome-dependent degradation of the transcriptional regulators ICE1 (Dong et al., 2006) and CO (Lazaro et al., 2012). However, SnRK1 protein levels in total protein extracts (Figure S4a,b) or cytoplasmic and nuclear fractions (Figure 3a–d) were not increased in *hos1*, indicating a non-proteolytic role of HOS1 in SnRK1 regulation. This is in accordance with reports of other HOS1 interactors that are regulated by HOS1 independently of its E3 ubiquitin ligase function (Han et al., 2020; Jung et al., 2013; Kim, Lee, Jung, et al., 2017; Lee et al., 2012). HOS1 is found in most land plants, but the RING finger domain is not always present, lacking for example in the HOS1 proteins of moss (*Physcomitrium patens*), common bean (*Phaseolus vulgaris*), and soybean (*Glycine max*) (Jung et al., 2014). In contrast, the NUP ELYS motif is

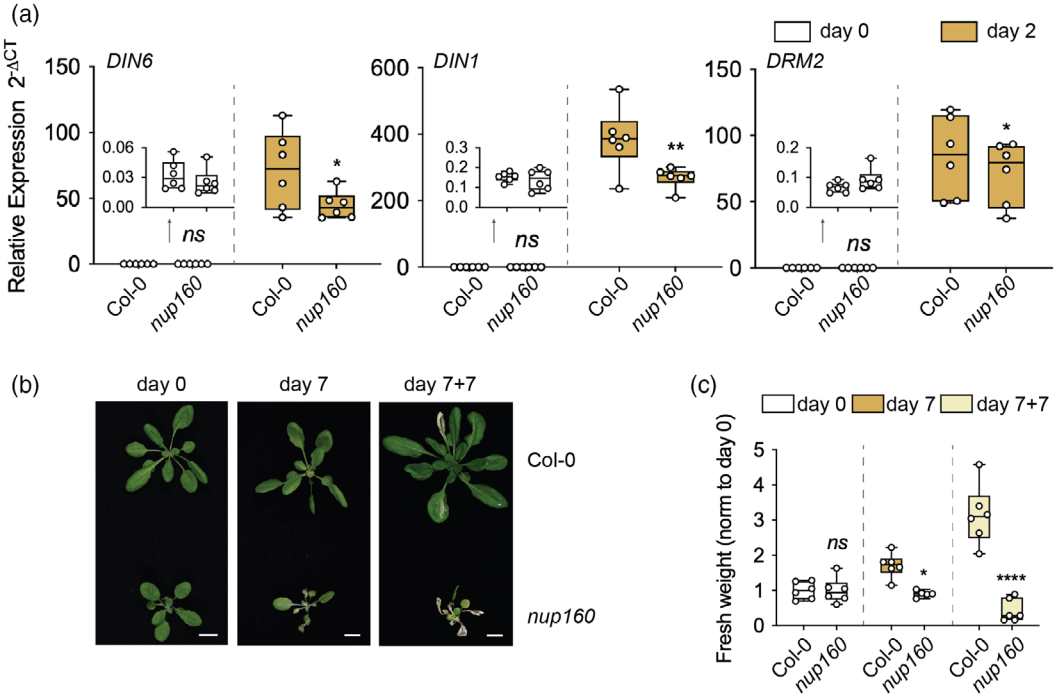

Figure 4. Tolerance of the NPC mutant *nup160* to prolonged darkness. (a) Induction of starvation genes (*DIN6*, *DIN1*, *DRM2*) measured by RT-qPCR from rosettes of 4-week-old Col-0 and *nup160* mutant plants collected on day 0 and after 2 days of dark treatment (day 2). Box and whisker plots represent six biological replicates (each consisting of one rosette per genotype and condition, grown in six independent batches). (b) Representative pictures of 4-week-old Col-0 and *nup160* plants (day 0) placed in constant darkness for 7 days (day 7) and transferred back to the initial photoperiod for 7 additional days (day 7 + 7). Scale bar = 1 cm. (c) Rosette fresh weight determined on days 0, 7, and 7 + 7 and normalized to day 0 for each genotype. Box and whisker plots represent five to six plants per genotype and condition (grown as three independent batches; note that the Col-0 set is the same as in Figure 1c). Asterisks denote statistically significant differences between Col-0 and *nup160* within each condition (days 0, 2, 7, and 7 + 7), as determined by two-way ANOVA with Sidak's multiple comparisons test. **P* < 0.05; ***P* < 0.01; *****P* < 0.0001; *ns*, non-significant.

ubiquitous and is highly conserved, suggesting that non-proteolytic roles of HOS1, in processes such as mRNA export and chromatin remodeling, could be more important than its E3 ubiquitin ligase activity (Jung et al., 2014; MacGregor et al., 2013). In this context, the fact that NLS-SnRK1α1 was able to rescue to a large extent the defects of *hos1* in low-energy responses (Figure 5c–e) suggests that at least one of the causes for these defects is the depletion of SnRK1α1 from the nucleus and that HOS1 is important for the nuclear accumulation of SnRK1α1. This interpretation is further supported by the molecular and plant phenotypes of the NPC mutant *nup160* in response to prolonged darkness (Figure 4), which are similar to those of *hos1*. Given that NUP160 is required for anchoring HOS1 to the NPC (Li et al., 2020), this indicates that SnRK1 signaling requires HOS1 localization at the NPC and/or an adequate NPC function. Supporting this, NUP160 was also recently identified as a SnRK1α1 interactor by TurboID-based proximity labeling (van Leene et al., 2022), and the double *nup160*/*hos1* mutant showed the same molecular and plant phenotypes in response to prolonged darkness as its parents (Figure S5). Altogether, this suggests that the HOS1 and NUP160 nucleoporins may act in concert to promote tolerance to low-energy stress via the SnRK1 kinase. Loss of HOS1 and/or NUP160 may impact the function and structural integrity of the NPC (Lüdke et al., 2021) and thereby cause reduced accumulation of SnRK1α1 in the nucleus of the respective mutant plants. The fact that the protein levels of the nucleoporin NUP96 are reduced in *hos1* (Cheng et al., 2020) suggests that the structural integrity of the NPC may indeed be compromised in this mutant. Furthermore, several NUPs, including NUP160, were shown to be important for the nucleo-cytoplasmic distribution of key regulators of auxin, salicylic acid, and defense signaling components (Cheng et al., 2009; Du et al., 2016; Parry et al., 2006), and HOS1 was recently implicated in the nuclear localization of the PIF4 transcription factor (Zhang et al., 2020). Depletion of the NUP ELYS, with a region of homology with HOS1, in human cells resulted in lower NPC density and reduced nuclear size (Jevtić et al., 2019), but normal nuclear size could be restored by overexpression of importin α, arguing that the impact of ELYS on nuclear size is import-mediated.

How HOS1 precisely interferes with the nuclear accumulation of SnRK1α1 awaits further mechanistic

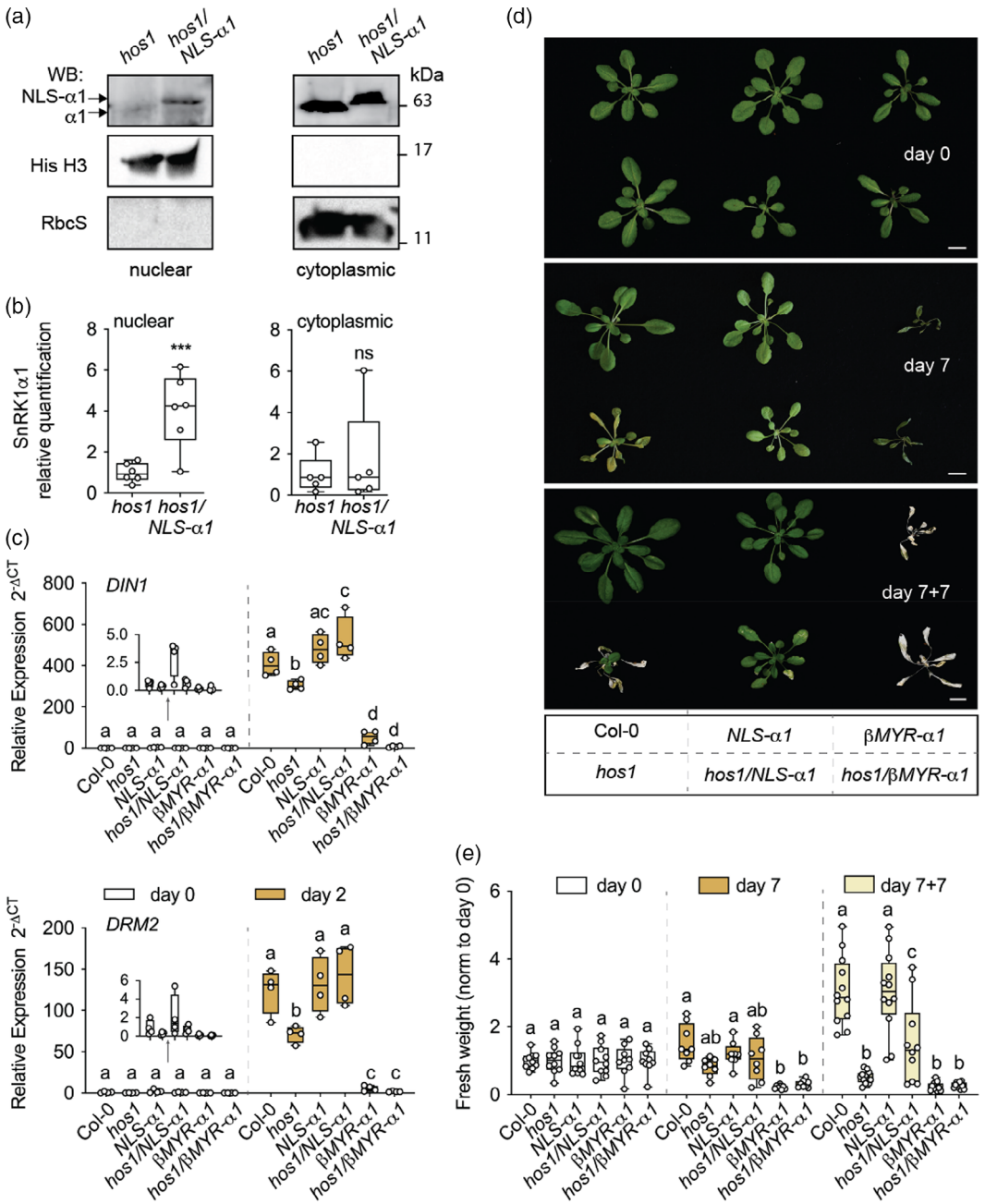

Figure 5. Impact of *NLS-SnRK1α1* in *hos1* tolerance to prolonged darkness. Cross between *hos1* and plants with predominant localization of SnRK1α1 in the nucleus (*NLS-SnRK1α1*, shown as *NLS-α1*) or outside the nucleus (*βMYR-SnRK1α1*, shown as *βMYR-α1*) (Ramon et al., 2019). (a) Nuclear fractionation from rosettes of 4-week-old *hos1* and *hos1*/*NLS-α1* plants. Representative WB of nuclear and cytoplasmic fractions with specific antibodies against SnRK1α1, histone 3 (His H3, nuclear marker, not detected in the WB image of the cytoplasmic fraction), and Rubisco small subunit (RbcS, cytosolic marker, not detected in the WB image of the nuclear fraction). Arrows point to SnRK1α1 (α1) or NLS-α1 proteins. (b) SnRK1α1 quantification normalized to His H3 in the nuclear fraction and to RbcS in the cytoplasmic fraction and further normalized to *hos1*. Box and whisker plots represent a minimum of five biological replicates, grown in a minimum of five independent batches. Asterisks denote statistically significant differences between *hos1* and *hos1*/*NLS-α1*, determined by a ratio paired *t*-test. ***$P < 0.001$; *ns*, non-significant. (c) Induction of starvation genes (*DIN1*, *DRM2*), as measured by RT-qPCR, in rosettes of 4-week-old plants of the indicated genotypes collected on day 0 and after 2 days of dark treatment (day 2). Box and whisker plots represent four biological replicates (each consisting of one rosette per genotype, grown in four independent batches). (d) Representative pictures of 4-week-old plants (day 0) of the indicated genotypes placed in constant darkness for 7 days (day 7) and transferred back to the initial photoperiod for 7 additional days (day 7 + 7). Scale bar = 1 cm. (e) Rosette fresh weight determined on days 0, 7, and 7 + 7 and normalized to day 0 for each genotype. Box and whisker plots represent 8–12 plants per genotype and condition (grown in four independent batches). Different letters denote statistically significant differences between genotypes within each condition (days 0, 2, 7, and 7 + 7), as determined by two-way ANOVA with Tukey's multiple comparisons test ($P < 0.05$).

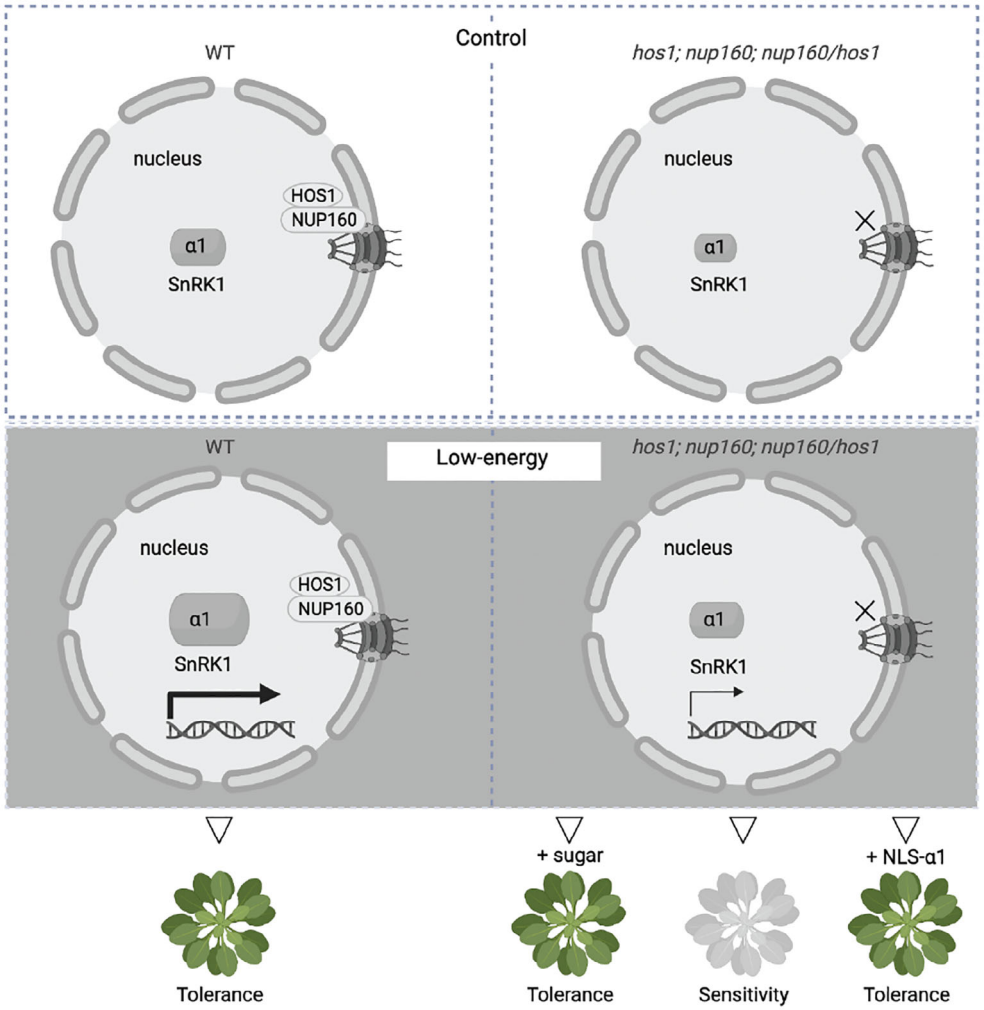

Figure 6. Model for the role of HOS1 in low-energy responses. In plants, low-energy conditions can derive from environmental stresses that impair photosynthesis or respiration. Plant tolerance to low energy availability relies on a central energy sensor and stress regulator, the SnRK1 protein kinase. The presence of the SnRK1 catalytic subunit SnRK1α1 in the nucleus is essential for the transcriptional reprogramming needed to balance energy levels (e.g., induction of 'starvation' genes). Depletion of the nuclear pore complex (NPC) component HOS1 causes constitutive defects in the nuclear accumulation of SnRK1α1. Accordingly, knockout mutants of HOS1 and NUP160, a nucleoporin that anchors HOS1 to the NPC, show compromised responses to low-energy stress. These defects can be largely reversed by sugar supplementation and through nuclear mobilization of SnRK1α1 via an *NLS-α1* transgene. Created with BioRender.com.

clarification. The SnRK1 regulator PLEIOTROPIC REGULATORY LOCUS 1 (PRL1; Bhalerao et al., 1999) interacts with IMPORTIN ALPHA 3 (IMPA3/MOS6; Németh et al., 1998), raising the possibility that nuclear import of SnRK1 is modulated by PRL1/IMPA3 interplay. It is possible that the physical interaction detected between HOS1 and SnRK1α1 (Figure 2a,b) could occur in the context of SnRK1α1 transport to the nucleus. The fact that the nuclear accumulation of PIF4 is compromised in the *hos1* mutant (Zhang et al., 2020) and that HOS1 interacts with PIF4 (Kim, Lee, Jung, et al., 2017) supports the view that HOS1 may contribute to the regulation of nuclear protein accumulation. It further suggests that this may occur through interaction with specific cargo proteins, such as PIF4 or SnRK1α1.

The reduced nuclear accumulation of SnRK1α1 in *hos1* causes defective induction of starvation genes and increased susceptibility to prolonged darkness, consistent with reports that nuclear SnRK1α1 is required for transcriptional responses and survival under low-energy conditions (Cho et al., 2012; Ramon et al., 2019). Like mammalian AMPK, which is translocated to the nucleus in response to several stress and hormonal stimuli (Kim et al., 2014; Kodiha et al., 2007; McGee et al., 2003; Suzuki et al., 2007), nuclear levels of SnRK1α1 were reported to increase under energy stress (Ramon et al., 2019), although such increase appeared to be specific to particular cell types (Blanco et al., 2019). In the case of *hos1*, nuclear accumulation of SnRK1α1 was constitutively reduced compared to Col-0,

both in light (Figure 3a,b) and dark stress conditions (Figure 3c,d). Similarly, the differences in the nuclear accumulation of IAA17 and PIF4 between Col-0 and *nup* mutants are constitutive, being quite prominent under control conditions. Although the differences are enhanced by heat stress, this enhancement is proportionally small when compared to the basal situation (Zhang et al., 2020). On the other hand, the fact that in *hos1* the reduced accumulation of SnRK1α1 in the nucleus is not accompanied by a proportional increase in the cytoplasmic fraction is to be expected, given that the nucleus constitutes a small percentage (approximately 8%) of the total cell volume (Huber & Gerace, 2007). Therefore, SnRK1α1 depletion from the *hos1* nucleus is expected to contribute little to the much larger cytoplasmic fraction, remaining undetectable.

Given the involvement of HOS1 in processes that are highly interconnected, it is not always possible to identify the primary defect caused by altered HOS1 function. SnRK1 has likewise been associated with a wide variety of processes, some of which, including hypocotyl elongation (Simon, Kusakina, et al., 2018; Simon, Sawkins, & Dodd, 2018), circadian function (Frank et al., 2018; Shin et al., 2017), and flowering time (Baena-González et al., 2007; Jeong et al., 2015; Sanagi et al., 2021; Tsai & Gazzarrini, 2012; Williams et al., 2014), are also affected by HOS1 (Kim, Lee, Jung, et al., 2017; Lazaro et al., 2012; MacGregor et al., 2013). A negative role in flowering regulation has been assigned to HOS1 and SnRK1α1, as shown by the early flowering phenotype of *hos1* (Lazaro et al., 2012) and by the delayed flowering of *SnRK1α1* overexpressor plants (Baena-González et al., 2007; Tsai & Gazzarrini, 2012; Williams et al., 2014). However, only the defects of *hos1* in the low-energy response but not in flowering could be rescued by increasing the levels of SnRK1α1 in the nucleus (Figure S6), showing that nuclear depletion of SnRK1α1 does not account for all the *hos1* phenotypes. It remains to be addressed whether the interaction between HOS1 and SnRK1 is of relevance for other processes, e.g., circadian clock function, where opposing roles have been reported for these factors (Frank et al., 2018; Shin et al., 2017).

In summary, we show that depletion of HOS1 leads to defective responses to low-energy stress that can be traced back to a constitutive reduction of SnRK1α1 levels in the nucleus (Figure 6). Altogether, our results demonstrate that the NPC component HOS1 is important for adequate SnRK1 signaling and thereby for plant tolerance to low-energy conditions.

EXPERIMENTAL PROCEDURES

All primers used in this study are provided in Table S1.

Plant material and growth conditions

Arabidopsis seeds were vapor-sterilized and stratified at 4°C for 2 days before sowing. Unless otherwise specified, plants were grown in soil under a 12 h light (100 μmol m^{-2} sec^{-1}) (22°C)/12 h dark (18°C) regime. All *Arabidopsis thaliana* plants used in this study are in the Col-0 background. The *hos1* (*hos1-3*, SALK_069312; *hos1-4*, EMS mutant; Lazaro et al., 2012), *nup160* (*nup160-4* or *sar1-4*, SALK_126801; Parry et al., 2006), *NLS-SnRK1α1* and *βMYR-SnRK1α1* (Ramon et al., 2019), and *snrk1α1* (*snrk1α1–3*, GABI_579E09; Crozet et al., 2016; Mair et al., 2015) lines have been previously described. The *hos1* mutant was crossed with *snrk1α1*, *nup160*, *NLS-SnRK1α1*, or *βMYR-SnRK1α1* to obtain the respective multiple mutant plants. To generate a *HOS1* complementation line (*35S::HOS1-GFP*/*hos1*), the coding sequence of *HOS1* (At2g39810.1) was amplified from leaf cDNA using the primers indicated in Table S1 and cloned into a pCB302-derived minibinary expression vector with a C-terminal GFP tag under the control of the 35S promoter (Baena-González et al., 2007). The construct was introduced into *Agrobacterium tumefaciens* GV3101 and *hos1* plants were transformed by the floral dip method (Clough & Bent, 1998). BASTA®-resistant transformants were selected based on their segregation ratio (T2) and homozygosity (T3).

In plate assays, for experiments involving sugar supply or when phenotyping the *nup160*/*hos1* mutant, sterilized seeds were plated in 0.5× MS Basal Medium (pH 5.7) with or without 1% sucrose as indicated and stratified at 4°C for 2 days. Plates were then transferred to the same equinoctial conditions as plants grown in soil (see above) for 12 days, prior to the dark stress treatments. Survival was scored at 7 + 7 days as the ability to retain chlorophyll in the shoot apex (as an indication of meristem viability) and the overall capacity to increase plant size and prevent desiccation.

Dark stress treatments

For plant material and growth conditions prior to treatment, refer to that specific section.

Short dark treatment (3 h): Fully expanded leaves of 4-week-old plants were detached from the rosettes at ZT6 and incubated on sterile MilliQ water in Petri dishes (three to four detached leaves, from a minimum of two rosettes) for 3 h under light (L) (control; 100 μmol m^{-2} sec^{-1}) or darkness (D, covered with aluminum foil). L and D samples were collected at ZT9 for gene expression analysis.

Extended night treatment (9 h): Two minutes before the start of the light period, 4-week-old Arabidopsis plants were either placed in a dark chamber at 22°C (constant temperature) or left under the regular conditions as controls. Rosettes were collected at ZT9 after 9 h of extended darkness (D) or control light treatment (L) for protein extraction and WB analysis.

Long dark treatment (2 days): Four-week-old Arabidopsis plants (day 0) were placed in constant darkness at a constant temperature (22°C) for 2 days (day 2). Rosettes collected at each time point were used for gene expression analyses.

Long dark treatment (7 days): Four-week-old Arabidopsis plants or 12-day-old seedlings (plate assays) were collected (day 0 samples) or placed in constant darkness at a constant temperature (22°C) for 7 days (day 7). Plants were then transferred back to the original conditions for recovery for 7 additional days (day 7 + 7). Rosettes collected at each time point were used for image acquisition and for measuring rosette fresh weight.

Yeast two-hybrid assays

The full-length coding sequence of *HOS1* (At2g39810.1) was cloned into pGADT7 in fusion with the GAL4 activation domain (AD). A pGBKT7 construct, harboring full-length *SnRK1α1* (At3g01090.1) fused to the DNA binding domain (BD) of GAL4, was also used. The empty vectors (EVs) were used as negative controls. Yeast cells (Y2HGold) were transformed with both pGADT7 and pGBKT7 constructs and yeast growth was assessed in low-stringency medium (−leucine [L]/−tryptophan [W]) for selection of co-transformants and in high-stringency medium (−L/−W/−histidine [H]/−adenine [A]) for selection of interactors.

(Co-)immunoprecipitation assays

Arabidopsis rosettes of 4-week-old plants (*35S::GFP* and *35S::HOS1-GFP*/*hos1*) were finely ground in liquid nitrogen. Proteins were extracted with IP buffer (1 ml g^{-1} fresh material) (50 mM Tris–HCl pH 8.0, 50 mM NaCl, 1% [v/v] Igepal CA-630, 0.5% [w/v] sodium deoxycholate, 0.1% [w/v] SDS, 1 mM EDTA pH 8.0, 50 μM MG132, 50 mM *N*-ethylmaleimide, cOmplete protease inhibitor cocktail [1 tablet per 20 ml, Roche, Basel, Switzerland, 11697498001], and 1:500 [v/v] phosphatase inhibitor 2 [Sigma P5726, St. Louis, Missouri, USA] and phosphatase inhibitor 3 [Sigma P0044, St. Louis, Missouri, USA]). After clearing samples by centrifugation (21 130 ***g*** at 4°C, 15 min), a small aliquot (30 μl) of each supernatant was taken and quantified using Pierce™ 660 nm assay reagent with ionic detergent compatibility reagent. The remaining supernatant was incubated at 4°C for 2 h under gentle rotation with 40 μl of μMACS anti-GFP MicroBeads (μMACS GFP Isolation Kit, Miltenyi, 130-091-125). Samples were thereafter loaded in μColumns (Miltenyi Biotec, 130-042-701, Bergish Gladbach, Germany) pre-equilibrated with 1 ml of IP buffer and allowed to flow through. Columns were washed four times with 200 μl of IP buffer and proteins were eluted with 80 μl of elution buffer (Miltenyi, 130-091-125) at 95°C. β-Mercaptoethanol (2%) was added to eluates and supernatant samples prior to boiling for 5 min at 95°C. Proteins were resolved by SDS-PAGE, wet-transferred to PVDF membranes (110 V, 1 h at 4°C), and immunodetected using anti-SnRK1α1 and anti-GFP antibodies.

Protein extraction

Arabidopsis rosettes of 4-week-old plants (Col-0, *hos1*, and *HOS1-GFP*/*hos1* complementation lines) were finely ground using a TissueLyser II (Qiagen, Hilden, Germany), and proteins were extracted using the IP buffer described in the '(Co-)immunoprecipitation assays' section (1,5 ml g^{-1} fresh material). After clearing samples by centrifugation (21 130 ***g*** at 4°C, 15 min), the supernatants were recovered, and total protein was quantified using Pierce™ 660 nm protein assay reagent with ionic detergent compatibility reagent. Samples were denatured using 4× Laemmli solubilization buffer and boiling for 5 min at 95°C. An equal protein amount per sample was loaded in the gels, and proteins were resolved by SDS-PAGE, wet-transferred to PVDF membranes (110 V, 1 h at 4°C), and immunodetected using antibodies against the indicated SnRK1 subunits or GFP (in the *GFP* and *HOS1-GFP*/*hos1* lines). Coomassie or Ponceau staining was used as protein loading control.

Nuclear fractionation

Arabidopsis rosettes of 4-week-old plants were finely ground in liquid nitrogen and transferred to 2-ml tubes. The sample powder was added to 3× (w/v) of Nuclear Isolation Buffer (NIB) (20 mM Tris–HCl pH 8.0, 250 mM sucrose, 5 mM $MgCl_2$, 5 mM KCl, 5 mM EDTA pH 8.0, 14 mM β-mercaptoethanol, 0.6% [v/v] Triton X-100, 1% [w/v] polyvinylpyrrolidone [PVP40], cOmplete protease inhibitor cocktail [1 tablet per 50 ml, Roche 11697498001], and 1:500 [v/v] phosphatase inhibitor 2 [Sigma P5726] and phosphatase inhibitor 3 [Sigma P0044]) and incubated under gentle rotation at 4°C for 15 min. Samples were then filtered through two layers of Miracloth® (Merck-Millipore, Burlington, Massachusetts, EUA; prewet with NIB) and centrifuged at 1240 ***g*** at 4°C for 10 min. The supernatant, corresponding to the cytoplasmic fraction, was thereafter separated from the nuclei (pellet). Nuclei were washed four times with 2 ml of NIB, carefully resuspending the pellets with a brush and centrifuging at 1240 ***g*** at 4°C for 10 min each time. Nuclei were then resuspended in 200 μl of NIB (bis) (20 mM Tris–HCl pH 8.0, 250 mM sucrose, 5 mM $MgCl_2$, 5 mM KCl, 5 mM EDTA pH 8.0, cOmplete protease inhibitor cocktail [1 tablet per 50 ml], and 1:500 [v/v] phosphatase inhibitor 2 and phosphatase inhibitor 3), added on top of 1 ml of a Percoll solution (15% [v/v] Percoll, 20 mM Tris–HCl pH 8.0, 250 mM sucrose, 5 mM $MgCl_2$, 5 mM KCl, 5 mM EDTA pH 8.0, cOmplete protease inhibitor cocktail [1 tablet per 50 ml], and 1:500 [v/v] phosphatase inhibitor 2 and phosphatase inhibitor 3) and centrifuged at 1240 ***g*** at 4°C for 10 min. Supernatants were thereafter discarded and nuclear pellets were mixed with 20 μl of 4× Laemmli buffer and boiled at 95°C for 15 min, with brief vortexing every 5 min. Cytoplasmic fractions collected in the beginning were quantified using Pierce™ 660 nm assay reagent with ionic detergent compatibility reagent. Equal protein amounts of cytoplasmic samples and whole nuclei samples were separated by 15% SDS-PAGE and analyzed with

anti-SnRK1α1, anti-histone H3, and anti-Rubisco small subunit (RbcS) antibodies by WB.

Antibodies and Western blot

The SnRK1α1 (1:4000) antibody was previously described (Belda-Palazón et al., 2020). Anti-SnRK1β1 (1:500, anti-AKINB1, AS09460) was purchased from Agrisera, Vannas, Sweden. Phospho-SnRK1α1/2 (T175/176) was detected with an anti-phospho-T172-AMPKα antibody (1:1000 in 5% BSA in Tris-buffered saline (TBS) with Tween, referred to as P-AMPK; #2535, Cell Signaling Technologies, Danvers, Massachusetts, USA). Histone H3 (1:5000, ab1791, Abcam, Cambridge, UK) and RbcS (1:5000, anti-RbcS, AS07 259, Agrisera, Vannas, Sweden) were used to characterize the nuclear and cytoplasmic fractions, respectively. The anti-GFP (1:1000, 11814460001, Roche) antibody was used to detect the corresponding tagged proteins. For WB, all primary antibodies were diluted in 1% non-fat milk in TBS (unless otherwise stated) and membranes were incubated with the antibodies under gentle shaking for 16 h at 4°C. After incubation with Peroxidase AffiniPure goat anti-rabbit or anti-mouse IgG (H + L; 1:10 000; Jackson ImmunoResearch) in 1% non-fat milk in TBS for 1 h at room temperature, chemiluminescence detection was performed using ECL Western Blotting Detection Reagent (GE Healthcare) and SuperSignal West Femto Maximum Sensitivity Substrate (Thermo Scientific).

Gene expression analyses

For RT-qPCR quantification of gene expression, RNA was extracted from detached leaves and rosettes of Arabidopsis plants using TRIzol Reagent (Ambion, Life Technologies). RNA was thereafter treated with RNase-Free DNase (Promega, Madison, Wisconsin, USA) and reverse transcribed (1 μg) using SuperScript III Reverse Transcriptase (Invitrogen, Waltham, Massachusetts, USA, ThermoFisher, Waltham, Massachusetts, USA), according to the manufacturer's instructions. RT-qPCR was performed using iTaq Universal SYBR Green Supermix (cat. No. 1725124, Bio-Rad, Hercules, California, USA) according to the manufacturer's instructions in a total volume of 10 μl. The PCR program comprised an initial denaturation step for 30 sec at 95°C and amplification by 40 cycles of 15 sec at 95°C and 1 min at 60°C. PCR was performed in an ABI QuantStudio 7 Real Time PCR machine (Applied Biosystems, Waltham, Massachusetts, USA). Expression values of *DIN6*, *DIN1*, and *DRM2* were normalized to the average mean of *UBC21* and *SAND* expression (Czechowski et al., 2005) using the $2^{-\Delta Ct}$ method for relative quantification (Livak & Schmittgen, 2001).

Flowering assay

The number of rosette leaves at flowering (with a stem height of approximately 1 cm) was assessed in several plants of the different genotypes analyzed grown in soil under a long-day regime (16 h light [100 μmol m^{-2} sec^{-1}] at 23°C/8 h dark at 18°C).

Statistical analyses

Box and whisker plots, violin plots, and scatter plots were used to represent the experimental results. In box and whisker plots, lower and upper box boundaries represent the first and third quartiles, respectively, horizontal lines mark the median, and whiskers mark the highest and lowest values. In scatter plots, bars represent the mean ± SEM. Dots represent individual data points. In the RT-qPCR plots, each data point refers to a whole rosette, with the exception of Figure S1, where it refers to a pool composed of three to four detached leaves from a minimum of two rosettes. Each experiment was treated as a batch within which the different genotypes were matched. Statistically significant differences between the different genotypes within each treatment or condition were assessed by a two-way 'randomized block' analysis of variance (ANOVA), followed by a Tukey or a Sidak multiple comparisons test, with a 95% confidence interval. In the fresh weight plots, each data point refers to a whole rosette. For each genotype, individual fresh weight values were normalized to the average fresh weight on day 0 of the same genotype. Statistically significant differences between the different genotypes within each treatment or condition were assessed by ordinary two-way ANOVA, with no matching or pairing selected, followed by a Tukey or a Sidak multiple comparisons test, with a 95% confidence interval. In the protein quantification plots, each data point refers to a normalized protein band. Each experiment was treated as a batch within which the different genotypes were matched. Statistically significant differences between the different genotypes were assessed by a ratio paired *t*-test, with a 95% confidence interval (two-tailed). In the rosette leaves violin plots, each data point refers to a whole rosette. No matching or pairing was performed. Statistically significant differences between the different genotypes were assessed by ordinary one-way ANOVA, followed by a Tukey multiple comparisons test, with a 95% confidence interval. In the survival plots, each bar represents the mean ± SEM of the survival rates, for each genotype in each condition, from at least eight independent assays. Each experiment was treated as a batch within which the different genotypes were matched, within each condition. Statistically significant differences between the different genotypes were assessed by either two-way ANOVA with Sidak multiple comparisons test or by ordinary one-way ANOVA, followed by a Tukey multiple comparisons test, with a 95% confidence interval. Plotting and statistical analyses were performed using GraphPad Prism 9 version 9.1.1 for MacOS (GraphPad Software, LLC).

ACCESSION NUMBERS

Sequence data from this article can be found in the Arabidopsis Genome Initiative database under the following accession numbers: *SnRK1α1*, At3g01090; *SnRK1α2*, At3g29160; *SnRK1β1*, At5g21170; *HOS1*, At2g39810; *NUP160*, At1g33410; *DIN6*, At3g47340; *DIN1*, At4g35770; *DRM2*, At2g33830; *UBC21*, At5g25760; *SAND*, At2g28390.

AUTHOR CONTRIBUTIONS

LM, AC, and EBG designed the research; LM, AE, BBP, and BP performed the experiments; LM and AE analyzed the data; EBG supervised the research; EBG and LM wrote the article with input from all coauthors.

ACKNOWLEDGMENTS

We thank Vera Nunes from the IGC Model Organism Unit/Plant Facility for excellent plant management and Filip Rolland for kindly providing the *NLS-SnRK1α1* and *βMYR-SnRK1α1* lines. This work was supported by FCT - Fundação para a Ciência e a Tecnologia, I.P., through GREEN-IT - Bioresources for Sustainability R&D Unit (UIDB/04551/2020, UIDP/04551/2020), by the LS4FUTURE Associated Laboratory (LA/P/0087/2020, PTDC/BIA-FBT/4942/2020, LISBOA-01-0145-FEDER-028128, PTDC/BIA-BID/32347/2017, EXPL/ASP-AGR/1329/2021, 2022.08339.PTDC, SFRH/BPD/116116/2016 [LM], PD/BD/114361/2016 [BP], and 2020.03177.CEECIND [EBG]), and by the European Union Horizon 2020 research and innovation program (Grant Agreement number: 867426 — ABA GrowthBalance — H2020-WF-2018-2020/H2020-WF-01-2018, awarded to BBP).

CONFLICT OF INTEREST STATEMENT

The authors declare no conflict of interest.

SUPPORTING INFORMATION

Additional Supporting Information may be found in the online version of this article.

Figure S1. Tolerance of *hos1* and a *HOS1-GFP* complementation line to darkness.

Figure S2. Tolerance of the *hos1-4* mutant to prolonged darkness.

Figure S3. Tolerance of *hos1* to prolonged darkness in the presence of sugar.

Figure S4. Accumulation of SnRK1 subunits in *hos1*.

Figure S5. Tolerance of the NPC mutants *hos1* and *nup160* to prolonged darkness.

Figure S6. Impact of an *NLS-SnRK1α1* transgene on the flowering phenotype of *hos1*.

REFERENCES

Baena-González, E. & **Hanson, J.** (2017) Shaping plant development through the SnRK1–TOR metabolic regulators. *Current Opinion in Plant Biology*, **35**, 152–157.

Baena-González, E., **Rolland, F.**, **Thevelein, J.M.** & **Sheen, J.** (2007) A central integrator of transcription networks in plant stress and energy signalling. *Nature*, **448**, 938–942.

Baena-González, E. & **Sheen, J.** (2008) Convergent energy and stress signalling. *Trends in Plant Science*, **13**, 474–482.

Belda-Palazón, B., **Adamo, M.**, **Valerio, C.**, **Ferreira, L.J.**, **Confraria, A.**, **Reis-Barata, D.** ***et al.*** (2020) A dual function of SnRK2 kinases in the regulation of SnRK1 and plant growth. *Nature Plants*, **6**, 1345–1353. Available from: https://doi.org/10.1038/s41477-020-00778-w

Belda-Palazón, B., **Costa, M.**, **Beeckman, T.**, **Rolland, F.** & **Baena-González, E.** (2022) ABA represses TOR and root meristem activity through nuclear exit of the SnRK1 kinase. *Proceedings of the National Academy of Sciences of the United States of America*, **119**, e2204862119. Available from: https://doi.org/10.1073/pnas.2204862119

Bhalerao, R.P., **Salchert, K.**, **Bakó, L.**, **Ökrész, L.**, **Szabados, L.**, **Muranaka, T.** ***et al.*** (1999) Regulatory interaction of PRL1 WD protein with *Arabidopsis* SNF1-like protein kinases. *Proceedings of the National Academy of Sciences of the United States of America*, **96**, 5322–5327. Available from: https://doi.org/10.1073/pnas.96.9.5322

Blanco, N.E., **Liebsch, D.**, **Guinea Díaz, M.**, **Strand, Å.** & **Whelan, J.** (2019) Dual and dynamic intracellular localization of Arabidopsis thaliana SnRK1.1. *Journal of Experimental Botany*, **70**, 2325–2338.

Branco-Price, C., **Kaiser, K.A.**, **Jang, C.J.H.**, **Larive, C.K.** & **Bailey-Serres, J.** (2008) Selective mRNA translation coordinates energetic and metabolic adjustments to cellular oxygen deprivation and reoxygenation in *Arabidopsis thaliana*. *The Plant Journal*, **56**, 743–755. Available from: https://doi.org/10.1111/j.1365-313X.2008.03642.x

Broeckx, T., **Hulsmans, S.** & **Rolland, F.** (2016) The plant energy sensor: evolutionary conservation and divergence of SnRK1 structure, regulation, and function. *Journal of Experimental Botany*, **67**, 6215–6252. Available from: https://doi.org/10.1093/jxb/erw416

Cheng, Y.T., **Germain, H.**, **Wiermer, M.**, **Bi, D.**, **Xu, F.**, **García, A.V.** ***et al.*** (2009) Nuclear pore complex component MOS7/Nup88 is required for innate immunity and nuclear accumulation of defense regulators in arabidopsis. *Plant Cell*, **21**, 2503–2516. Available from: https://doi.org/10.1105/tpc.108.064519

Cheng, Z., **Zhang, X.**, **Huang, P.**, **Huang, G.**, **Zhu, J.**, **Chen, F.** ***et al.*** (2020) Nup96 and HOS1 are mutually stabilized and gate CONSTANS protein level, conferring long-day photoperiodic flowering regulation in Arabidopsis. *Plant Cell*, **32**, 374–391.

Cho, H.Y., **Loreti, E.**, **Shih, M.C.** & **Perata, P.** (2021) Energy and sugar signalling during hypoxia. *New Phytologist*, **229**, 57–63. Available from: https://doi.org/10.1111/nph.16326

Cho, Y.-H., **Hong, J.-W.**, **Kim, E.-C.** & **Yoo, S.-D.** (2012) Regulatory functions of SnRK1 in stress-responsive gene expression and in plant growth and development. *Plant Physiology*, **158**, 1955–1964.

Clough, S.J. & **Bent, A.F.** (1998) Floral dip: a simplified method forAgrobacterium-mediated transformation of Arabidopsis thaliana. *The Plant Journal*, **16**, 735–743. Available from: https://doi.org/10.1046/j.1365-313x.1998.00343.x

Col, V.d., **Fuchs, P.**, **Nietzel, T.** ***et al.*** (2017) ATP sensing in living plant cells reveals tissue gradients and stress dynamics of energy physiology. *eLife*, **6**, e26770.

Cookson, S.J., **Yadav, U.P.**, **Klie, S.**, **Morcuende, R.**, **Usadel, B.**, **Lunn, J.E.** ***et al.*** (2016) Temporal kinetics of the transcriptional response to carbon depletion and sucrose readdition in *Arabidopsis* seedlings. *Plant, Cell & Environment*, **39**, 768–786. Available from: https://doi.org/10.1111/pce.12642

Crozet, P., **Margalha, L.**, **Butowt, R.**, **Fernandes, N.**, **Elias, C.A.**, **Orosa, B.** ***et al.*** (2016) SUMOylation represses SnRK1 signalling in Arabidopsis. *The Plant Journal*, **85**, 120–133. Available from: https://doi.org/10.1111/tpj.13096

Czechowski, T., **Stitt, M.**, **Altmann, T.**, **Udvardi, M.K.** & **Scheible, W.-R.** (2005) Genome-wide identification and testing of superior reference genes for transcript normalization in Arabidopsis. *Plant Physiology*, **139**, 5–17.

Dong, C.H., **Agarwal, M.**, **Zhang, Y.**, **Xie, Q.** & **Zhu, J.K.** (2006) The negative regulator of plant cold responses, HOS1, is a RING E3 ligase that mediates the ubiquitination and degradation of ICE1. *Proceedings of the National Academy of Sciences of the United States of America*, **103**, 8281–8286. Available from: https://doi.org/10.1073/pnas.0602874103

Dröge-Laser, W. & **Weiste, C.** (2018) The C/S1 bZIP network: a regulatory hub orchestrating plant energy homeostasis. *Trends in Plant Science*, **23**, 422–433.

Du, J., **Gao, Y.**, **Zhan, Y.** ***et al.*** (2016) Nucleocytoplasmic trafficking is essential for BAK1- and BKK1-mediated cell-death control. *The Plant Journal*, **85**, 520–531. Available from: https://doi.org/10.1111/tpj.13125

Emanuelle, S., **Hossain, M.I.**, **Moller, I.E.**, **Pedersen, H.L.**, **van de Meene, A.M.L.**, **Doblin, M.S.** ***et al.*** (2015) SnRK1 from *Arabidopsis thaliana* is an atypical AMPK. *The Plant Journal*, **82**, 183–192. Available from: https://doi.org/10.1111/tpj.12813

Frank, A., **Matiolli, C.C.**, **Viana, A.J.C.**, **Hearn, T.J.**, **Kusakina, J.**, **Belbin, F.E.** ***et al.*** (2018) Circadian entrainment in Arabidopsis by the sugar-Responsive transcription factor bZIP63. *Current Biology*, **28**, 2597–2606.e6.

Gutierrez-Beltran, E. & **Crespo, J.L.** (2022) Compartmentalization, a key mechanism controlling the multitasking role of the SnRK1 complex E. Baena-González, ed. *Journal of Experimental Botany*, **73**, 7055–7067.

Han, S.-H., **Park, Y.-J.** & **Park, C.-M.** (2020) HOS1 activates DNA repair systems to enhance plant thermotolerance. *Nature Plants*, **6**, 1439–1446.

Henninger, M., **Pedrotti, L.**, **Krischke, M.**, **Draken, J.**, **Wildenhain, T.**, **Fekete, A.** ***et al.*** (2022) The evolutionarily conserved kinase SnRK1 orchestrates resource mobilization during Arabidopsis seedling establishment. *Plant Cell*, **34**, 616–632.

Huber, M.D. & **Gerace, L.** (2007) The size-wise nucleus: nuclear volume control in eukaryotes. *Journal of Cell Biology*, **179**, 583–584. Available from: https://doi.org/10.1083/jcb.200710156

Hulsmans, S., **Rodriguez, M.**, **de Coninck, B.** & **Rolland, F.** (2016) The SnRK1 energy sensor in plant biotic interactions. *Trends in Plant Science*, **21**, 648–661.

Ishitani, M., **Xiong, L.**, **Lee, H.**, **Stevenson, B.** & **Zhu, J.-K.** (1998) *HOS1*, a genetic locus involved in cold-Responsive gene expression in Arabidopsis. *Plant Cell*, **10**, 1151–1161.

Jamsheer, K.M., **Sharma, M.**, **Singh, D.**, **Mannully, C.T.**, **Jindal, S.**, **Shukla, B.N.** ***et al.*** (2018) FCS-like zinc finger 6 and 10 repress SnRK1 signalling in Arabidopsis. *The Plant Journal*, **94**, 232–245. Available from: https://doi.org/10.1111/tpj.13854

Jamsheer, K.M., **Kumar, M.** & **Srivastava, V.** (2021) SNF1-related protein kinase 1: the many-faced signalling hub regulating developmental plasticity in plants J. Lunn, ed. *Journal of Experimental Botany*, **72**, 6042–6065.

Jeong, E.-Y., **Seo, P.J.**, **Woo, J.C.** & **Park, C.-M.** (2015) AKIN10 delays flowering by inactivating IDD8 transcription factor through protein phosphorylation in Arabidopsis. *BMC Plant Biology*, **15**, 110. Available from: https://doi.org/10.1186/s12870-015-0503-8

Jevtić, P., **Schibler, A.C.**, **Wesley, C.C.**, **Pegoraro, G.**, **Misteli, T.** & **Levy, D.L.** (2019) The nucleoporin ELYS regulates nuclear size by controlling NPC number and nuclear import capacity. *EMBO Reports*, **20**, e47283. Available from: https://doi.org/10.15252/embr.201847283

Jung, J.-H., **Lee, H.-J.**, **Park, M.-J.** & **Park, C.-M.** (2014) Beyond ubiquitination: proteolytic and nonproteolytic roles of HOS1. *Trends in Plant Science*, **19**, 538–545.

Jung, J.-H., **Park, J.-H.**, **Lee, S.**, **To, T.K.**, **Kim, J.-M.**, **Seki, M.** ***et al.*** (2013) The cold Signalling attenuator HIGH EXPRESSION OF OSMOTICALLY RESPONSIVE GENE1 activates *FLOWERING LOCUS C* transcription via chromatin remodeling under short-term cold stress in *Arabidopsis*. *Plant Cell*, **25**, 4378–4390.

Jung, J.-H., **Seo, P.J.** & **Park, C.-M.** (2012) The E3 ubiquitin ligase HOS1 regulates Arabidopsis flowering by mediating CONSTANS degradation under cold stress. *Journal of Biological Chemistry*, **287**, 43277–43287.

Kim, J.-H., **Lee, H.-J.**, **Jung, J.-H.**, **Lee, S.** & **Park, C.-M.** (2017) HOS1 facilitates the Phytochrome B-mediated inhibition of PIF4 function during hypocotyl growth in Arabidopsis. *Molecular Plant*, **10**, 274–284.

Kim, J.-H., **Lee, H.-J.** & **Park, C.-M.** (2017) HOS1 acts as a key modulator of hypocotyl photomorphogenesis. *Plant Signaling & Behavior*, **12**, e1315497. Available from: https://doi.org/10.1080/15592324.2017.1315497

Kim, N., **Lee, J.O.**, **Lee, H.J.**, **Lee, S.K.**, **Moon, J.W.**, **Kim, S.J.** ***et al.*** (2014) AMPKα2 translocates into the nucleus and interacts with hnRNP H: implications in metformin-mediated glucose uptake. *Cellular Signalling*, **26**, 1800–1806.

Kodiha, M., **Rassi, J.G.**, **Brown, C.M.** & **Stochaj, U.** (2007) Localization of AMP kinase is regulated by stress, cell density, and signalling through the MEK→ERK1/2 pathway. *American Journal of Physiology-Cell Physiology*, **293**, C1427–C1436. Available from: https://doi.org/10.1152/ajpcell.00176.2007

Lazaro, A., **Mouriz, A.**, **Piñeiro, M.** & **Jarillo, J.A.** (2015) Red light-mediated degradation of CONSTANS by the E3 ubiquitin ligase HOS1 regulates photoperiodic flowering in Arabidopsis. *Plant Cell*, **27**, 2437–2454.

Lazaro, A., **Valverde, F.**, **Piñeiro, M.** & **Jarillo, J.A.** (2012) The *Arabidopsis* E3 ubiquitin ligase HOS1 negatively regulates CONSTANS abundance in the photoperiodic control of flowering. *Plant Cell*, **24**, 982–999.

Lee, H., **Xiong, L.**, **Gong, Z.**, **Ishitani, M.**, **Stevenson, B.** & **Zhu, J.-K.** (2001) The *Arabidopsis HOS1* gene negatively regulates cold signal transduction and encodes a RING finger protein that displays cold-regulated nucleo–cytoplasmic partitioning. *Genes & Development*, **15**, 912–924. Available from: https://doi.org/10.1101/gad.866801

Lee, J.H., **Kim, J.J.**, **Kim, S.H.**, **Cho, H.J.**, **Kim, J.** & **Ahn, J.H.** (2012) The E3 ubiquitin ligase HOS1 regulates low ambient temperature-Responsive flowering in Arabidopsis thaliana. *Plant & Cell Physiology*, **53**, 1802–1814. Available from: https://doi.org/10.1093/pcp/pcs123

Lee, K. & **Seo, P.J.** (2015a) The Arabidopsis E3 ubiquitin ligase HOS1 contributes to auxin biosynthesis in the control of hypocotyl elongation. *Plant Growth Regulation*, **76**, 157–165. Available from: https://doi.org/10.1007/s10725-014-9985-x

Lee, K. & **Seo, P.J.** (2015b) The E3 ubiquitin ligase HOS1 is involved in ethylene regulation of leaf expansion in *Arabidopsis*. *Plant Signaling & Behavior*, **10**, e1003755. Available from: https://doi.org/10.1080/15592324.2014.1003755

Li, C., **Liu, L.**, **Teo, Z.W.N.**, **Shen, L.** & **Yu, H.** (2020) Nucleoporin 160 regulates flowering through anchoring HOS1 for destabilizing CO in Arabidopsis. *Plant Communications*, **1**, 100033.

Li, X. & **Gu, Y.** (2020) Structural and functional insight into the nuclear pore complex and nuclear transport receptors in plant stress signalling. *Current Opinion in Plant Biology*, **58**, 60–68.

Livak, K.J. & **Schmittgen, T.D.** (2001) Analysis of relative gene expression data using real-time quantitative PCR and the $2-\Delta\Delta CT$ method. *Methods*, **25**, 402–408.

Lüdke, D., **Rohmann, P.F.W.** & **Wiermer, M.** (2021) Nucleocytoplasmic communication in healthy and diseased plant tissues. *Frontiers in Plant Science*, **12**, 719453. Available from: https://doi.org/10.3389/fpls.2021.719453

MacGregor, D.R., **Gould, P.**, **Foreman, J.**, **Griffiths, J.**, **Bird, S.**, **Page, R.** ***et al.*** (2013) HIGH EXPRESSION OF OSMOTICALLY RESPONSIVE GENES1 is required for circadian periodicity through the promotion of Nucleocytoplasmic mRNA export in Arabidopsis. *Plant Cell*, **25**, 4391–4404.

MacGregor, D.R. & **Penfield, S.** (2015) Exploring the pleiotropy of hos1. *Journal of Experimental Botany*, **66**, 1661–1671. Available from: https://doi.org/10.1093/jxb/erv022

Mair, A., **Pedrotti, L.**, **Wurzinger, B.**, **Anrather, D.**, **Simeunovic, A.**, **Weiste, C.** ***et al.*** (2015) SnRK1-triggered switch of bZIP63 dimerization mediates the low-energy response in plants. *eLife*, **4**, 1–33.

Margalha, L., **Confraria, A.** & **Baena-González, E.** (2019) SnRK1 and TOR: modulating growth–defense trade-offs in plant stress responses. *Journal of Experimental Botany*, **70**, 2261–2274.

McGee, S.L., **Howlett, K.F.**, **Starkie, R.L.**, **Cameron-Smith, D.**, **Kemp, B.E.** & **Hargreaves, M.** (2003) Exercise increases nuclear AMPK α2 in human skeletal muscle. *Diabetes*, **52**, 926–928.

Miura, K., **Jin, J.B.**, **Lee, J.**, **Yoo, C.Y.**, **Stirm, V.**, **Miura, T.** ***et al.*** (2007) SIZ1-mediated Sumoylation of ICE1 controls *CBF3/DREB1A* expression and freezing tolerance in *Arabidopsis*. *Plant Cell*, **19**, 1403–1414.

Miura, K., **Ohta, M.**, **Nakazawa, M.**, **Ono, M.** & **Hasegawa, P.M.** (2011) ICE1 Ser403 is necessary for protein stabilization and regulation of cold signalling and tolerance. *The Plant Journal*, **67**, 269–279. Available from: https://doi.org/10.1111/j.1365-313X.2011.04589.x

Muhammad, I., **Shalmani, A.**, **Ali, M.**, **Yang, Q.-H.**, **Ahmad, H.** & **Li, F.B.** (2021) Mechanisms regulating the dynamics of photosynthesis under abiotic stresses. *Frontiers in Plant Science*, **11**, 615942. Available from: https://doi.org/10.3389/fpls.2020.615942

Németh, K., **Salchert, K.**, **Putnoky, P.**, **Bhalerao, R.**, **Koncz-Kálmán, Z.**, **Stankovic-Stangeland, B.** ***et al.*** (1998) Pleiotropic control of glucose and hormone responses by PRL1, a nuclear WD protein, in *Arabidopsis*. *Genes & Development*, **12**, 3059–3073. Available from: https://doi.org/10.1101/gad.12.19.3059

Nukarinen, E., **Nägele, T.**, **Pedrotti, L.**, **Wurzinger, B.**, **Mair, A.**, **Landgraf, R.** ***et al.*** (2016) Quantitative phosphoproteomics reveals the role of the AMPK plant ortholog SnRK1 as a metabolic master regulator under energy deprivation. *Scientific Reports*, **6**, 31697.

Nunes, C., **Primavesi, L.F.**, **Patel, M.K.**, **Martinez-Barajas, E.**, **Powers, S.J.**, **Sagar, R.** ***et al.*** (2013) Inhibition of SnRK1 by metabolites: tissue-dependent effects and cooperative inhibition by glucose 1-phosphate in combination with trehalose 6-phosphate. *Plant Physiology and Biochemistry*, **63**, 89–98.

Parry, G., **Ward, S.**, **Cernac, A.**, **Dharmasiri, S.** & **Estelle, M.** (2006) The *Arabidopsis* SUPPRESSOR OF AUXIN RESISTANCE proteins are nucleoporins with an important role in hormone Signalling and development. *Plant Cell*, **18**, 1590–1603.

Pedrotti, L., **Weiste, C.**, **Nägele, T.**, **Wolf, E.**, **Lorenzin, F.**, **Dietrich, K.** ***et al.*** (2018) Snf1-RELATED KINASE1-controlled C/S $_1$ -bZIP Signalling activates alternative mitochondrial metabolic pathways to ensure plant survival in extended darkness. *Plant Cell*, **30**, 495–509.

Peixoto, B., **Moraes, T.A.**, **Mengin, V.**, **Margalha, L.**, **Vicente, R.**, **Feil, R.** ***et al.*** (2021) Impact of the SnRK1 protein kinase on sucrose homeostasis and the transcriptome during the diel cycle. *Plant Physiology*, **187**, 1357–1373.

Ramon, M., **Dang, T.V.T.**, **Broeckx, T.**, **Hulsmans, S.**, **Crepin, N.**, **Sheen, J.** ***et al.*** (2019) Default activation and nuclear translocation of the plant cellular energy sensor SnRK1 regulate metabolic stress responses and development. *Plant Cell*, **31**, 1614–1632.

Ramon, M., **Ruelens, P.**, **Li, Y.**, **Sheen, J.**, **Geuten, K.** & **Rolland, F.** (2013) The hybrid four-CBS-domain KINβγ subunit functions as the canonical γ subunit of the plant energy sensor SnRK1. *The Plant Journal*, **75**, 11–25. Available from: https://doi.org/10.1111/tpj.12192

Sanagi, M., **Aoyama, S.**, **Kubo, A.**, **Lu, Y.**, **Sato, Y.**, **Ito, S.** ***et al.*** (2021) Low nitrogen conditions accelerate flowering by modulating the phosphorylation state of FLOWERING BHLH 4 in *Arabidopsis*. *Proceedings of the National Academy of Sciences of the United States of America*, **118**, e2022942118. Available from: https://doi.org/10.1073/pnas.2022942118

Seo, P.J., **Jung, J.-H.**, **Park, M.-J.**, **Lee, K.** & **Park, C.-M.** (2013) Controlled turnover of CONSTANS protein by the HOS1 E3 ligase regulates floral transition at low temperatures. *Plant Signaling & Behavior*, **8**, e23780. Available from: https://doi.org/10.4161/psb.23780

Shen, W., **Reyes, M.I.** & **Hanley-Bowdoin, L.** (2009) Arabidopsis protein kinases GRIK1 and GRIK2 specifically activate SnRK1 by phosphorylating its activation loop. *Plant Physiology*, **150**, 996–1005.

Shin, J., **Sánchez-Villarreal, A.**, **Davis, A.M.**, **Du, S.**, **Berendzen, K.W.**, **Koncz, C.** ***et al.*** (2017) The metabolic sensor AKIN10 modulates the *Arabidopsis* circadian clock in a light-dependent manner. *Plant, Cell & Environment*, **40**, 997–1008. Available from: https://doi.org/10.1111/pce.12903

Simon, N.M.L., **Kusakina, J.**, **Fernández-López, Á.**, **Chembath, A.**, **Belbin, F.E.** & **Dodd, A.N.** (2018) The energy-Signalling hub SnRK1 is important for sucrose-induced hypocotyl elongation. *Plant Physiology*, **176**, 1299–1310.

Simon, N.M.L., **Sawkins, E.** & **Dodd, A.N.** (2018) Involvement of the SnRK1 subunit KIN10 in sucrose-induced hypocotyl elongation. *Plant Signaling & Behavior*, **13**, e1457913. Available from: https://doi.org/10.1080/15592324.2018.1457913

Sugden, C., **Donaghy, P.G.**, **Halford, N.G.** & **Hardie, D.G.** (1999) Two SNF1-related protein kinases from spinach leaf phosphorylate and inactivate 3-Hydroxy-3-Methylglutaryl-coenzyme a Reductase, nitrate Reductase, and sucrose phosphate synthase in Vitro1. *Plant Physiology*, **120**, 257–274.

Sun, D., **Fang, X.**, **Xiao, C.**, **Ma, Z.**, **Huang, X.**, **Su, J.** ***et al.*** (2021) Kinase SnRK1.1 regulates nitrate channel SLAH3 engaged in nitrate-dependent alleviation of ammonium toxicity. *Plant Physiology*, **186**, 731–749. Available from: https://doi.org/10.1093/plphys/kiab057

Suzuki, A., **Okamoto, S.**, **Lee, S.**, **Saito, K.**, **Shiuchi, T.** & **Minokoshi, Y.** (2007) Leptin stimulates fatty acid oxidation and peroxisome proliferator-activated receptor α gene expression in mouse C2C12 myoblasts by changing the subcellular localization of the α2 form of AMP-activated protein kinase. *Molecular and Cellular Biology*, **27**, 4317–4327. Available from: https://doi.org/10.1128/MCB.02222-06

Tamura, K., **Fukao, Y.**, **Iwamoto, M.**, **Haraguchi, T.** & **Hara-Nishimura, I.** (2011) Identification and characterization of nuclear pore complex components in *Arabidopsis thaliana*. *Plant Cell*, **22**, 4084–4097.

Tomé, F., **Nagele, T.**, **Adamo, M.** ***et al.*** (2014) The low energy signalling network. *Frontiers in Plant Science*, **5**, 1–12. Available from: https://doi.org/10.3389/fpls.2014.00353

Tsai, A.Y.-L. & **Gazzarrini, S.** (2012) AKIN10 and FUSCA3 interact to control lateral organ development and phase transitions in Arabidopsis. *The Plant Journal*, **69**, 809–821. Available from: https://doi.org/10.1111/j.1365-313X.2011.04832.x

van Leene, J., **Eeckhout, D.**, **Gadeyne, A.** ***et al.*** (2022) Mapping of the plant SnRK1 kinase signalling network reveals a key regulatory role for the class II T6P synthase-like proteins. *Nature Plants*, **8**, 1245–1261.

Wang, B., **Duan, C.-G.**, **Wang, X.**, **Hou, Y.-J.**, **Yan, J.**, **Gao, C.** ***et al.*** (2015) HOS1 regulates Argonaute1 by promoting transcription of the microRNA gene *MIR168b* in Arabidopsis. *The Plant Journal*, **81**, 861–870. Available from: https://doi.org/10.1111/tpj.12772

Williams, S.P., **Rangarajan, P.**, **Donahue, J.L.**, **Hess, J.E.** & **Gillaspy, G.E.** (2014) Regulation of sucrose non-Fermenting related kinase 1 genes in Arabidopsis thaliana. *Frontiers in Plant Science*, **5**, 1–13. Available from: https://doi.org/10.3389/fpls.2014.00324

Yuan, S., **Zhang, Z.-W.**, **Zheng, C.**, **Zhao, Z.Y.**, **Wang, Y.**, **Feng, L.Y.** ***et al.*** (2016) *Arabidopsis* cryptochrome 1 functions in nitrogen regulation of flowering. *Proceedings of the National Academy of Sciences of the United States of America*, **113**, 7661–7666. Available from: https://doi.org/10.1073/pnas.1602004113

Zhai, Z., **Keereetaweep, J.**, **Liu, H.**, **Feil, R.**, **Lunn, J.E.** & **Shanklin, J.** (2018) Trehalose 6-phosphate positively regulates fatty acid synthesis by stabilizing WRINKLED1. *Plant Cell*, **30**, 2616–2627.

Zhang, A., **Wang, S.**, **Kim, J.**, **Yan, J.**, **Yan, X.**, **Pang, Q.** ***et al.*** (2020) Nuclear pore complex components have temperature-influenced roles in plant growth and immunity. *Plant, Cell & Environment*, **43**, 1452–1466. Available from: https://doi.org/10.1111/pce.13741

Zhang, Y., **Primavesi, L.F.**, **Jhurreea, D.**, **Andralojc, P.J.**, **Mitchell, R.A.C.**, **Powers, S.J.** ***et al.*** (2009) Inhibition of SNF1-related protein Kinase1 activity and regulation of metabolic pathways by Trehalose-6-phosphate. *Plant Physiology*, **149**, 1860–1871.

Zhu, Y., **Wang, B.**, **Tang, K.**, **Hsu, C.-C.**, **Xie, S.**, **Du, H.** ***et al.*** (2017) An Arabidopsis nucleoporin NUP85 modulates plant responses to ABA and salt stress Z.-M. Pei, ed. *PLoS Genetics*, **13**, e1007124. Available from: https://doi.org/10.1371/journal.pgen.1007124